Bull. Mater. Sci., Vol. 29, No. 4, August 2006, pp. 403–411. © Indian Academy of Sciences.

# Gas sensing properties of Cu and Cr activated BST thick films

**G H JAIN and L A PATIL***

P.G. Department of Physics, Pratap College, Amalner 425 401, India

MS received 17 April 2006; revised 16 June 2006

**Abstract.** **$H_2S$ gas sensing properties of BST ($(Ba_{0.67}Sr_{0.33})TiO_3$) thick films are reported here for the first time. BST ceramic powder was prepared by mechanochemical process. Thick films of BST were prepared by screen-printing technique. The sensing performance of the films was tested for various gases. The films were surface customized by dipping them into aqueous solutions of $CuCl_2$ and $CrO_3$ for various intervals of time. These surface modified BST films showed improved sensitivity to $H_2S$ gas (100 ppm) than pure BST film. Chromium oxide was observed to be a better activator than copper oxide in $H_2S$ gas sensing. The effect of microstructure and amount of activators on $H_2S$ gas sensing were discussed. The sensitivity, selectivity, stability, response and recovery time of the sensor were measured and presented.**

**Keywords.** **$(Ba_{0.67}Sr_{0.33})TiO_3$ thick films; chromination; cuprication; $H_2S$ gas sensor; sensitivity; selectivity.**

## 1. Introduction

In the recent past sensors have attracted a great deal of attention from scientists and engineers. Even in the near future it is expected to gain importance in view of the construction of more or less intelligent ensembles, which integrate actuating, sensing and computing subsystems (Mair 1993). Detection of various gases using solid-state chemistry has generated a great deal of interest, both in academia and in industry (Hirschfeld *et al* 1986).

Although much research has been focused on sensors based on $SnO_2$ technology, other inorganic oxides are receiving increased attention. These include binary oxides, such as oxides of titanium, tungsten, and gallium, and more complex ternary oxides (Meisuer and Lampe 1995). Compounds having perovskite structures are among one of the most important classes of ternary oxides. Barium titanate ($BaTiO_3$) is one of the most intensively investigated ferroelectrics and has been widely used in electronic industry in applications for capacitors, thermocouples, transducers, sensors and actuators, etc (Herbert 1980; Setter and Collar 1993). A number of studies have focused on the chemistry and physics of the response of these materials to gases. Depending on the conditions, these compounds can behave as *n*- or *p*-type semiconductors. Because of their structural similarity, similar mechanisms of interaction with gases are expected to occur for these compounds, although the relative importance of the mechanisms for any specific operating condition would depend, in each instance, on the specific compound.

*Author for correspondence (lapresearch@rediffmail.com)

An approach of using these materials as sensors is to operate them at sufficiently high temperatures so that the thermodynamically controlled structural changes are induced by ambient gas concentrations. Thus, changes in the crystal structure of the material induced by the analyte are primarily responsible for changes in physical properties that are transduced into an appropriate electrical signal. At lower temperatures, changes in ambient gas concentration do not necessarily lead to equilibrium of the internal structure of the material, but can affect electrical properties through surface reactions.

Furthermore, some composite systems such as (Ba, Sr) $TiO_3$ and (Ba, Pb) $TiO_3$ ceramics have been studied to broaden the application of $BaTiO_3$-based thermisters for wider temperature range (Kim *et al* 2001; Lee *et al* 2002). Recently, $SrTiO_3$- and $BaTiO_3$-based sensors have received much attention because of their multisensing properties such as humidity, thermal and photosensitivities (Li *et al* 2000). Generally speaking, they possess good properties such as chemical and thermal stability, environmental adaptability and wide range of working temperature.

BST, a well known member of the perovskite family of oxides, has been studied for quite some time. Thin films of BST are considered to be a potential candidate for tunable microwave devices (Jain *et al* 2003), IR sensors (Zhu *et al* 2004), and also as chemical sensors for sensing of humidity (Agarwal *et al* 2001) and gas (Zhu *et al* 2000; Roy *et al* 2005). Although much progress has been made on application related to other areas, the gas sensing properties of BST thin films have not been explored for any gas other than hydrogen (Zhu *et al* 2000) and ammonia (Roy *et al* 2005).

In this paper, we report for the first time, $H_2S$ gas sensing phenomena observed in screen-printed BST thick films. The surface resistance of thick films decreases when exposed to $H_2S$ gas. Some of the well known materials for $H_2S$ gas sensing are $SnO_2$–ZnO–CuO (Ishihara *et al* 1995), $SnO_2$–Pd (Liao *et al* 2001), $SnO_2$–$Al_2O_3$ (Haeusler and Meyer 1996), $SnO_2$–CuO (Kanefusa *et al* 1985; Lantto and Romppainen 1988; Tamaki *et al* 1992; Manorama *et al* 1994; Wagh *et al* 2004; Patil and Patil 2006), $SnO_2$–CuO–$SnO_2$ (Sarala Devi *et al* 1995), $ZnSb_2O_6$ (Tamaki *et al* 1998) and $BaTiO_3$ (Jain *et al* 2005). Many researchers have developed various types of sensors by adding additives (Yamazoe *et al* 1983; Ishihara *et al* 1995; Lee and Meyer 2000; Haeusler and Meyer 1996) into base material for making the sensor material semiconducting to improve the sensing performance. The additive can be incorporated in the material either by doping or dipping technique. The dipping technique was adopted in the present study to incorporate Cu and Cr additives into BST thick films.

The studies on structural, micro-structural, elemental analysis and thermal stability of BST were carried out. The sensing performance of the sensors was tested using static gas sensing system.

## 2. Experimental

### 2.1 *Preparation of BST powder*

The AR grade powders of $Ba(OH)_2 8H_2O$, $Sr(OH)_2$ (with 2 : 1 molar concentration) and $TiO_2$ were ball milled to mix thoroughly followed by sintering at 1000°C for 6 h (Manku 1984; Lee 2002). The fine-grained powder was obtained by milling in planetary ball mill for 2 h. The XRD spectrum of as prepared powder confirmed the crystalline perovskite phase. The Ba/Sr composition ratio of the as prepared powder was confirmed to be 2 : 1 in the microarea EDS analysis.

### 2.2 *Preparation of BST thick films*

The thixotropic paste was formulated by mixing the fine powder of BST with a solution of ethyl cellulose (a temporary binder) in a mixture of organic solvents such as butyl cellulose, butyl carbitol acetate, terpineol, etc. The ratio of the inorganic to organic part was kept at 75 : 25 in formulating the paste. This paste was screen printed on a glass substrate in a desired pattern (Patil *et al* 1998, 1999). The films were fired at 550°C for 30 min.

### 2.3 *Surface modification of BST thick films*

The CuO-modified and $Cr_2O_3$-modified BST thick films were obtained by dipping them, respectively in 0·01M aqueous solution of copper chloride ($CuCl_2$) and 0·1M aqueous solution of chromium trioxide ($CrO_3$) for different intervals of dipping time: 5, 10, 20 and 30 min. These films were dried at 80°C, followed by firing at 550°C for 30 min. The films so prepared are termed as 'surface cupricated' and 'surface chrominated' films (Aslam *et al* 1999; Chaudhary *et al* 1999; Niranjan *et al* 2001; Jain *et al* 2005; Wagh *et al* 2006).

### 2.4 *Thickness measurements*

The thickness of the films was measured by using the Taylor–Hobson (Talystep, UK) system. The thicknesses of the films were observed in the range from 65–70 μm. The reproducibility in thickness of the films was possible by maintaining proper rheology and thixotropy of the paste.

### 2.5 *Details of gas sensing system*

The sensing performance of the sensors was examined using the 'static gas sensing system' (figure 1). There were electrical feeds through the base plate. The heater was fixed on the base plate to heat the sample under test up to desired operating temperature. The current passing through the heating element was monitored using a relay operated with an electronic circuit with adjustable ON–OFF time intervals. The Cr–Al thermocouple was used to sense the operating temperature of the sensor. The output of the thermocouple was connected to a digital temperature indicator. A gas inlet valve was fitted at one of the ports of the base plate. The required gas concentration inside the static system was achieved by injecting a known volume of a test gas using a gas-injecting syringe. A constant voltage was applied to the sensor, and the current was measured by a digital picoammeter. Air was allowed to pass into the glass chamber after every gas exposure cycle.

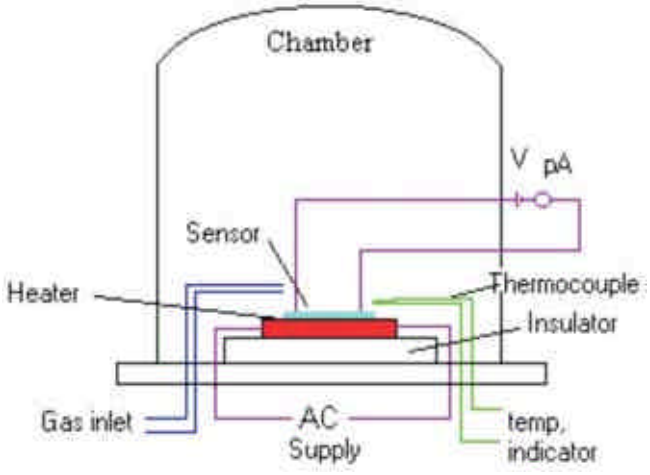


**Figure 1.** The block diagram of the gas sensing system.

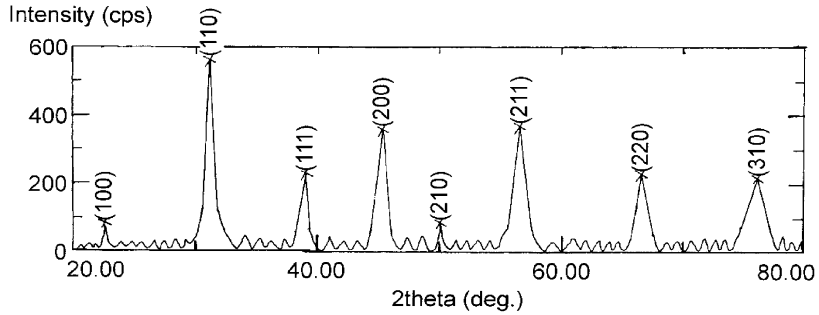


**Figure 2.** X-ray diffractogram of a BST thick film.

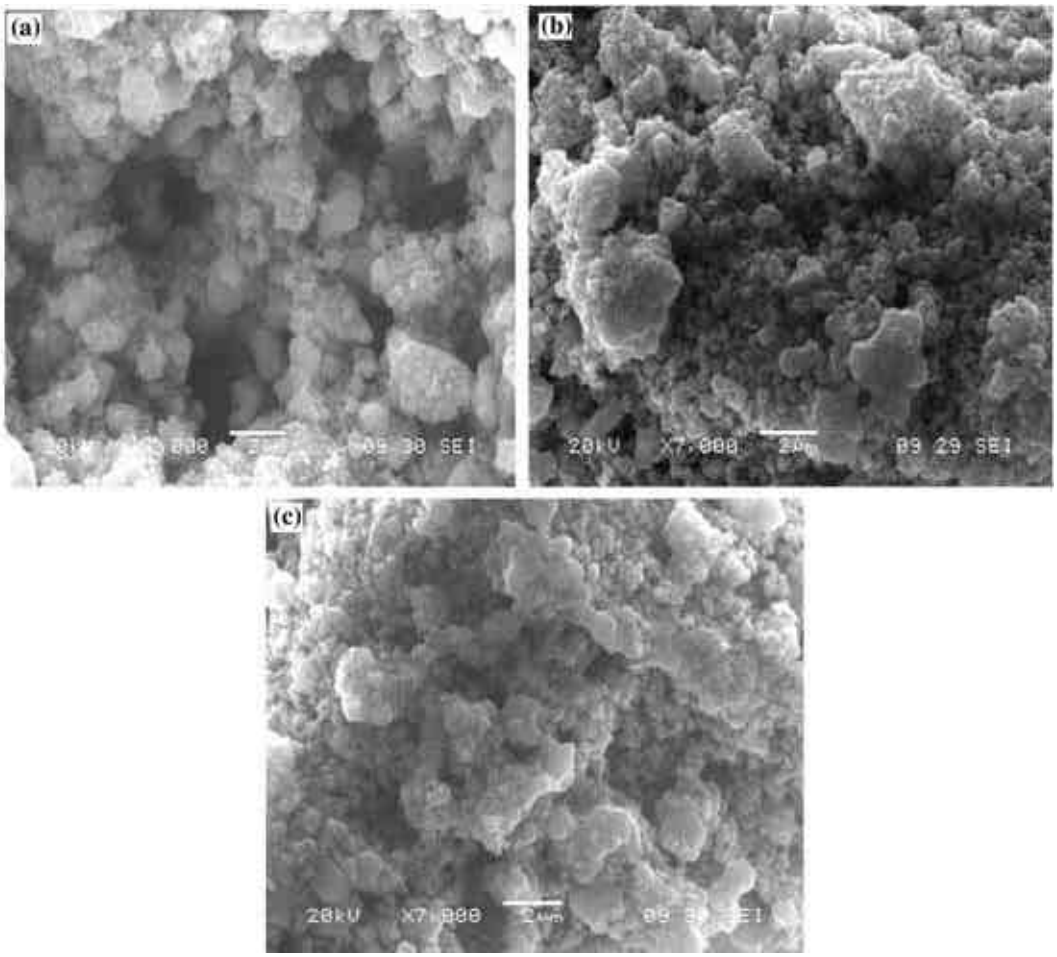


**Figure 3.** SEM images of (**a**) pure BST, (**b**) cupricated BST and (**c**) chrominated BST films.

## 3. Results

### 3.1 *X-ray diffraction studies*

X-ray studies of the thick films were carried out using a Philips X-ray diffractometer (model PW-1730). Figure 2 shows the X-ray diffractogram of a BST thick film.

The observed peaks match well with the reported ASTM data of BST, confirming the single phase of the compound. The average grain size was determined by using Scherrer formula and was estimated to be 484 nm.

### 3.2 *Microstructural analysis*

Scanning electron microscopic (SEM) studies were carried out using JEOL 6300(LA), Japan. Figures 3(a)–(c) depict SEM images of an unmodified, cupricated and chromi-

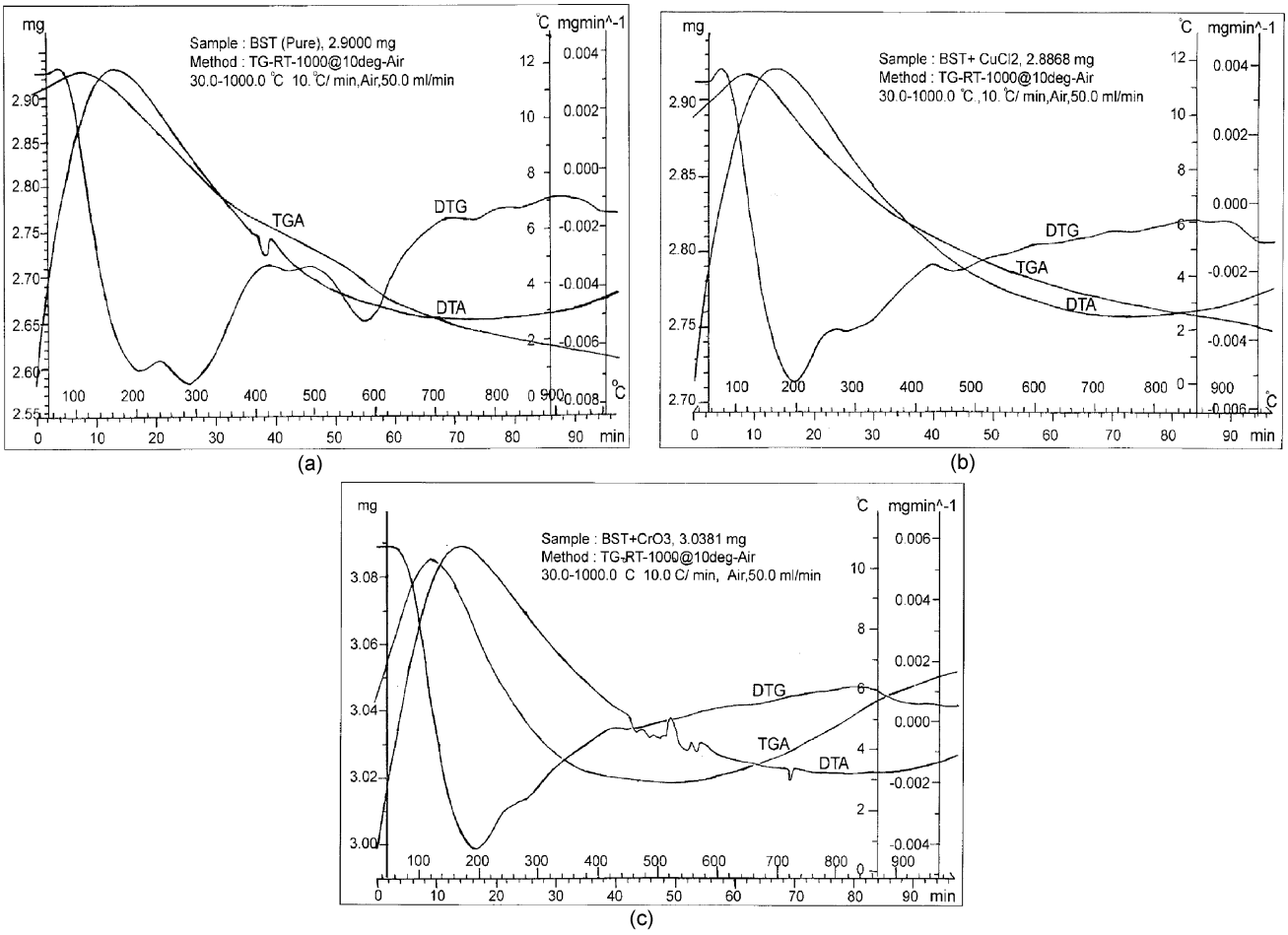


**Figure 4.** TGA, DTG and DTA of (**a**) pure BST, (**b**) cupricated BST and (**c**) chrominated BST.

nated BST thick films, respectively fired at 550°C. The unmodified film consists of voids and large grains with grain sizes ranging from 300–2000 nm distributed non-uniformly. The micrograph of cupricated (20 min) film shows a number of small particles distributed uniformly between the larger grains of BST, which may be attributed to the presence of CuO. The micrograph of chrominated (20 min) film shows a number of small particles distributed uniformly between the larger grains around BST, which may be attributed to the presence of $Cr_2O_3$.

### 3.3 *Elemental analysis of modified films*

The elemental analysis of the films was carried out using an energy dispersive spectrometer (EDS) JEOL, JED-2300, Japan. The constituent elements such as Ba, Sr, Ti, O, Cu and Cr associated with various films are given in table 1.

It is clear from the table that the weight percentage of copper increases with dipping time, reaches to a maximum (20 min) and then decreases with a further increase in dipping time interval with an oxygen deficiency of 7·60 wt%. The weight percentage of chromium goes on increasing with dipping time. The chrominated film with dipping time of 20 min was observed to have an oxygen deficiency of 6·87 wt%. Oxygen deficiency would be favourable for adsorption of more oxygen species.

### 3.4 *Thermal stability of pure, cupricated and chrominated BST*

Thermogravimetric (TGA), differential thermal (DTA) and derivative thermogravimetric (DTG) analyses of pure, cupricated and surface chrominated samples were carried out using Mettler Toledo Star System-851 under same condition in static air, and their profiles are given in figures 4 a–c, respectively.

Table 2 lists losses or gains in weight of pure, cupricated and chrominated BST in the different ranges of temperature as observed from TGA. It can be concluded from the profiles that the modified samples are observed to be more stable than pure. Also the chrominated sample is more stable than the cupricated one. The variation in weight with temperature was presented by DTG at a high resolution. The DTA showed endothermic nature of reac-

**Table 1.** Quantitative elemental analysis.

| Sample | | Wt % of Ba | Sr | Ti | O | Cu | Cr |
|---|---|---|---|---|---|---|---|
| Unmodified BST | | 54·08 | 15·88 | 22·44 | 7·90 | – | – |
| Cupricated BST | – Dipping time: 5 min | 52·40 | 16·44 | 22·36 | 8·61 | 0·21 | – |
| | – Dipping time: 10 min | 54·95 | 15·73 | 22·12 | 6·96 | 0·23 | – |
| | – Dipping time: 20 min | 53·17 | 15·82 | 22·41 | 7·60 | 1·0 | – |
| | – Dipping time: 30 min | 53·16 | 15·58 | 23·06 | 7·67 | 0·53 | – |
| Chrominated BST | – Dipping time: 5 min | 49·21 | 17·94 | 24·48 | 7·77 | – | 0·61 |
| | – Dipping time: 10 min | 52·50 | 15·78 | 23·33 | 7·75 | – | 0·65 |
| | – Dipping time: 20 min | 53·34 | 15·86 | 23·22 | 6·87 | – | 0·71 |
| | – Dipping time: 30 min | 52·10 | 16·67 | 22·11 | 8·20 | – | 0·91 |

**Table 2.** Thermal analyses.

| Pure BST | | | Cupricated BST | | | Chrominated BST | | |
|---|---|---|---|---|---|---|---|---|
| Temperature (°C) | Loss (wt%) | Gain (wt%) | Temperature (°C) | Loss (wt%) | Gain (wt%) | Temperature (°C) | Loss (wt%) | Gain (wt%) |
| 30–115 | – | 1·5 | 30–125 | – | 1·1 | 30–125 | 1·5 | – |
| 115–1000 | 11 | – | 125–1000 | 4·8 | – | 125–480 | 2·15 | – |
| | | | | | | 480–550 | Constant | Constant |
| | | | | | | 550–1000 | – | 1·05 |

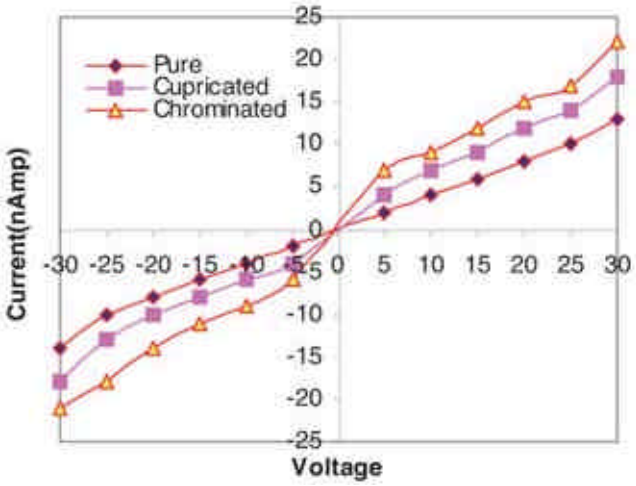


**Figure 5.** *I–V* characteristics of the BST thick films.

tions for both pure and modified BST. The heat absorbed by the samples may be due to the non-stoichiometry of BST and oxygen deficiency. Comparatively more gain in chrominated sample (as compared to pure and cupricated sample) can be attributed to the larger amount of adsorption of oxygen. The $Cr_2O_3$ misfits on the surface chrominated sample would act as efficient catalysts for oxygenation.

### 3.5 *Electrical properties*

3.5a *I–V characteristics:* Figure 5 shows the *I–V* characteristics of pure and chrominated BST thick film in air atmosphere. The linearity in the graphs indicate the ohmic nature of the silver contacts.

3.5b *Dependence of electrical conductivity on temperature:* Figure 6 represents the variation of conductivity with temperature for the pure, cupricated and chrominated samples. The dotted lines with open symbols are the graphs for samples tested in air atmosphere, while the dotted lines with solid symbols represent the graphs for the conductivities in the presence of $H_2S$ gas (100 ppm). The conductivity varied linearly with temperature for all samples showing the semiconducting nature. The conductivity of cupricated and chrominated samples upon exposure to gas was larger than that in air. The conductivity of the sample chrominated for 20 min was largest of all in gas ambient.

### 3.6 *Measurement of sensor response*

Sensitivity of a sensor is defined as the ratio of change in conductance of the sample on exposure to a test gas to the conductance in air.

$$\text{Sensitivity} = \frac{Gg - Ga}{Ga} = \frac{\Delta G}{Ga},$$

where $Gg$ and $Ga$ are the conductances of a sample in the presence and absence of a test gas, respectively, and $\Delta G$ the change in conductance.

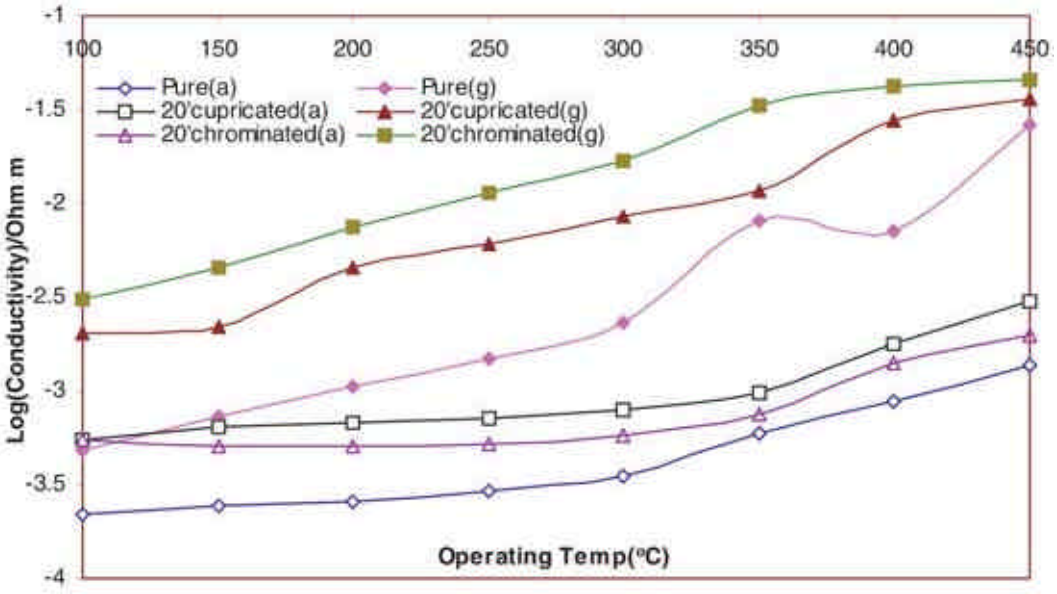


**Figure 6.** Variation of electrical conductivity with temperature. Open symbols represent the data in air and solid symbols are for 100 ppm $H_2S$ gas.

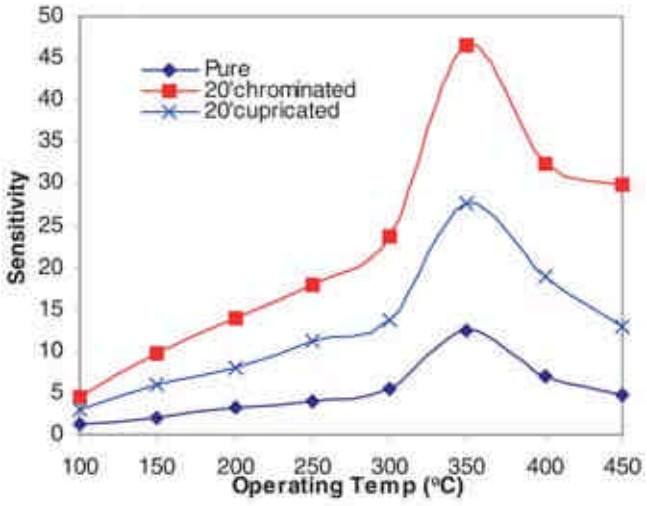


**Figure 7.** Variations in sensitivity to $H_2S$ gas (100 ppm) with operating temperature.

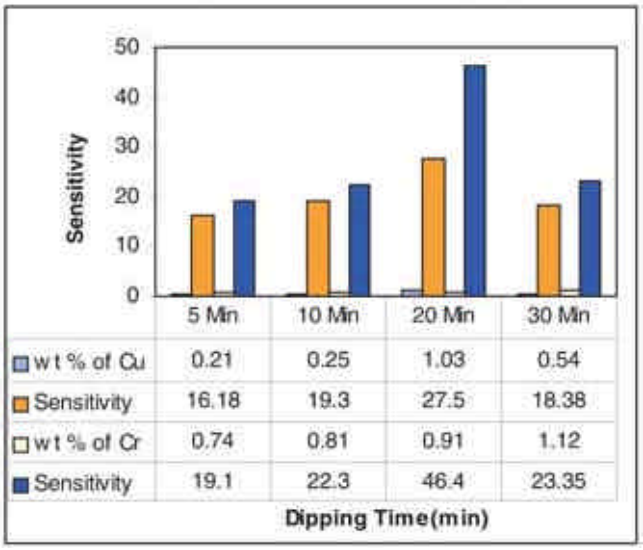


**Figure 8.** Variation in sensitivity to $H_2S$ with dipping time.

The sensitivity values of unmodified (pure), cupricated and surface chrominated BST films were determined at various operating temperatures ranging from 100–450°C. Figure 7 shows variations in sensitivity to $H_2S$ gas (100 ppm) with operating temperature of the unmodified and modified (cupricated and chrominated) BST films fired at 550°C. The sensitivity goes on increasing with increase in operating temperature, attains its maximum (at 350°C) and then decreases with a further increase in operating temperature. It is clear from the figure that the optimum operating temperature is 350°C.

The $H_2S$ sensitivity of unmodified BST fired at 550°C was 12·52 at 350°C, while sensitivity values of surface cupricated and chrominated BST(20 min) were 27·5 and 46·4, respectively, at the same operating temperature. Therefore, the surface chromination of BST was observed to be more effective in $H_2S$ gas sensing than the unmodified and cupricated BST samples.

### 3.7 *Variation of sensitivity with dipping time*

Figure 8 shows histogram indicating the sensitivity (to $H_2S$ gas) of the cupricated and chrominated films treated

for different intervals of time. The sensitivity to $H_2S$ goes on increasing with increase of Cr, attains its maximum at 0·91 wt% and decreases further. The chrominated sample treated for 20 min was observed to be most sensitive. The amount of Cr (0·91 wt%) incorporated onto BST surface would be optimum to cover the surface uniformly, leading to enhanced adsorption. The largest sensitivity, in case of the sample with 0·91 wt% of chromium (for 20 min), may be due to optimum number of chromium misfits on the surface for the oxygen to be adsorbed and in turn to oxidize the test gas.

### 3.8 *Selectivity of chrominated BST to various gases*

The ability of a sensor to respond to a certain gas in the presence of other gases is known as selectivity.

Figure 9 shows the bar diagram indicating the selectivity of the pure, cupricated and chrominated BST sensor operated at 350°C to $H_2S$ gas against $NH_3$, $H_2$, CO, ethanol, $CO_2$ and LPG gases. It is evident from the figure that the chrominated sensor was highly selective to $H_2S$ gas against $NH_3$, $H_2$, CO, ethanol, $CO_2$ and LPG gases. Selectivity of film would be improved due to surface modification. The high selectivity to $H_2S$ can be attributed to the surface modification (chromination) of BST films.

### 3.9 *Response and recovery time of sensors*

The time taken for the sensor to attain 80% of maximum change in resistance upon exposure to gas is the response time. The time taken by the sensor to get back 80% to the original resistance is the recovery time (Ishihara *et al* 1991). Response and recovery times of the sensor were measured. Figure 10 shows the variations in response to $H_2S$ gas with time in seconds for the chrominated BST films operated during 100°C through 450°C and fired at 550°C. The 80% response and recovery levels were attained within 3 and 9 s, respectively. The very short response and recovery time is the important feature of the chrominated BST.

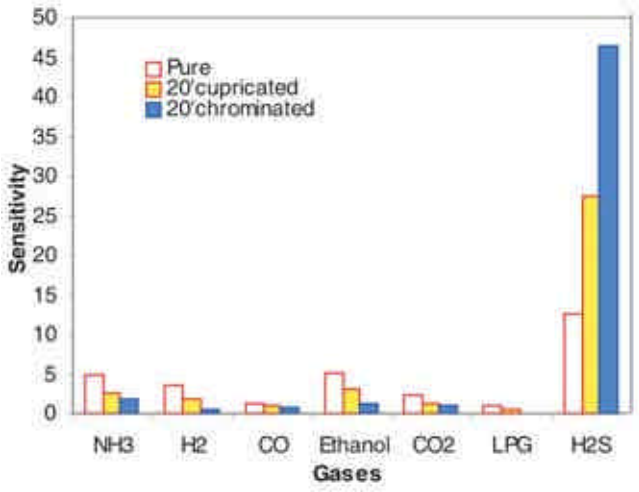


**Figure 9.** Selectivity of chrominated BST to various gases.

## 4. Discussion

The BST film surfaces were modified with $CuCl_2$ and $CrO_3$ using dipping technique. The $CuCl_2$ and $CrO_3$ would be converted into CuO and $Cr_2O_3$ during the firing of the films. These films can be looked upon as the small particles of surface activators (CuO and $Cr_2O_3$) distributed along the grain boundaries of base material and would occupy the intergrain spaces which develop the new surface sites beneficial for improvement of gas response and selectivity of a particular gas.

The gas response of Cr-modified films was observed to be larger than the gas response of Cu-modified BST films. This may be explained as follows:

The ionic radius of chromium (0·62 Å) is smaller than copper (0·73 Å). Therefore, the segregation of Cr ions would be easier than Cu ions into the base material and could occupy more surface sites as compared to Cu ions. The adsorption–desorption process would be more effective in case of Cr-activated films as compared to the Cu-activated films.

The Cr and Cu activators can create artificial surface states in the midgap region, leading to unusual physical and chemical properties. For example, the adsorption energy can be higher for the misfit regions, and the discontinuity in the adsorption potential can give rise to unusual selectivity effects for BST based semiconducting

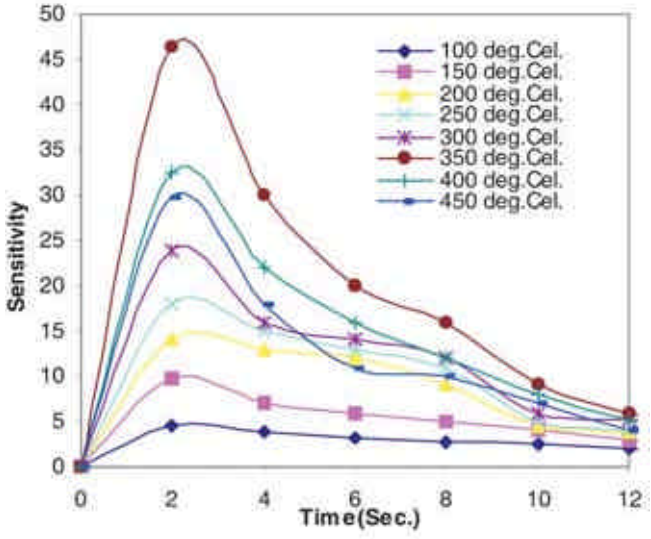


**Figure 10.** Transient response of chrominated BST to $H_2S$ gas.

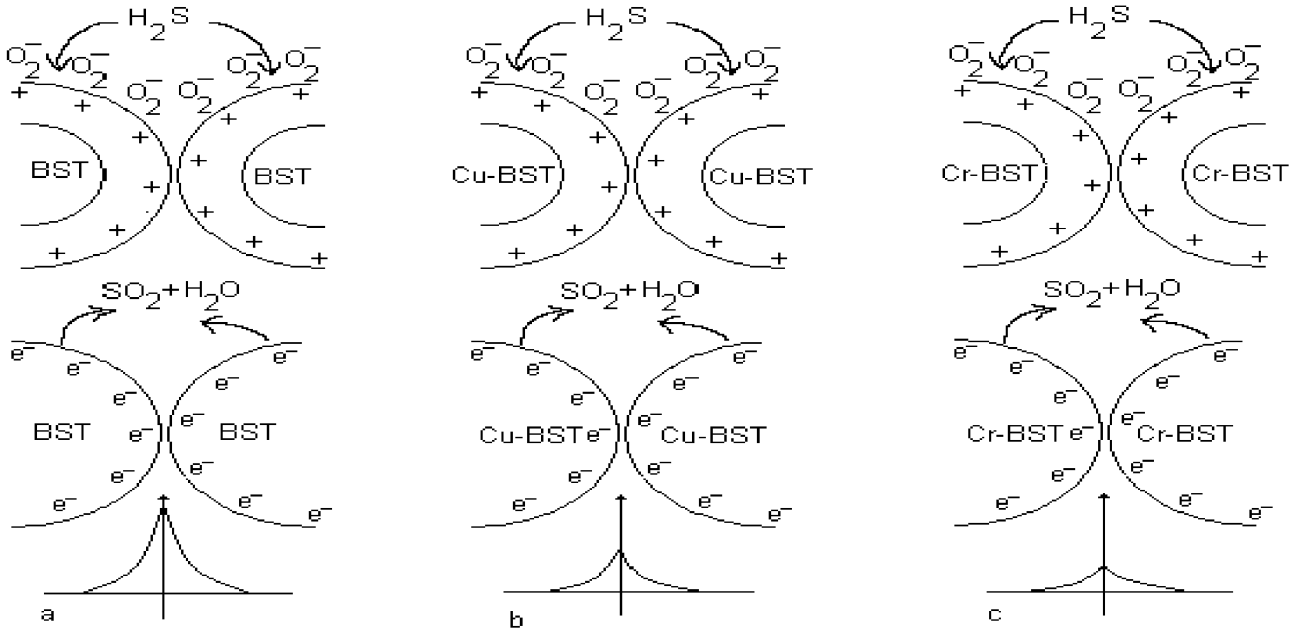


**Figure 11.** Gas sensing mechanism of (**a**) pure, (**b**) cupricated and (**c**) chrominated BST sensors to $H_2S$ gas.

oxide sensors. More specifically, the electron–electron interaction in the presence of periodically enhanced disorders in these two-dimensional systems can create the adsorbate–adsorbent interaction and the range of adsorption potentials leading to additional sensitivity improvement.

It is also observed from SEM pictures that the grains associated in Cr-activated films are smaller and more spherical as compared to the grains associated with the unmodified films. Therefore, the effective surface area in case of activated films would be larger than the unmodified films. This enables the faster adsorption–desorption process and therefore, faster response and recovery in case of modified films.

The chemical reactions responsible to enhance conductivity of the modified Cu and Cr added BST films could be represented as

$$Cr_2O_3 + 3H_2S \rightarrow Cr_2S_3 + 3H_2O, \quad (1)$$

$$CuO + H_2S \rightarrow CuS + H_2O. \quad (2)$$

$Cr_2S_3$ and CuS are known to be metallic and conducting in nature. Due to the reduction of oxides into sulphides, the film resistance would decrease suddenly. Upon subsequent exposure of sensor to air ambient at elevated temperatures, sulphides got oxidized and could be recovered back to oxides as

$$2Cr_2S_3 + 9O_2 \rightarrow 2Cr_2O_3 + 6SO_2, \quad (3)$$

$$2CuS + 4O_2 \rightarrow 2CuO + 2SO_3. \quad (4)$$

Figure 11 shows the adsorption of oxygen species on the surface of BST, abstracting electrons, and thus, causing an increase in potential barrier at the grain boundaries. When reducing gas such as $H_2S$, comes into contact with the grains of BST, the potential barrier would decrease as a result of oxidative conversion of $H_2S$ gas and desorption of oxygen.

The reaction of $H_2S$ with the adsorbed oxygen ions can be represented as

$$2H_2S + 3O_2^- \rightarrow 2H_2O + 2SO_2 + 6e^-. \quad (5)$$

The potential barrier height in case of chrominated sample (figure 11c) on exposure to gas would decrease as compared to pure and cupricated BST samples. This can be attributed to larger Cr-misfit regions on the surface. Larger the misfits on the surface, larger would be the number of species adsorbed on the surface and faster the oxidation of $H_2S$ gas.

## 5. Conclusions

Following conclusions can be drawn from the experimental results:

(I) Surface modification process was employed to modify only the surface of the film and not the bulk portion of the base material (BST).
(II) The chrominated and cupricated BST was observed to be semiconducting in nature and showed a negative temperature coefficient of resistance.
(III) The sensing mechanism of the surface modified BST was the surface-controlled mechanism (adsorption/desorption).
(IV) The oxidation of sulphides ($Cr_2S_3$, CuS) and the re-

duction of oxides ($Cr_2O_3$, CuO) have also boosted the gas response and selectivity.

(V) Chromium oxide would form larger number of misfits on the surface region than cuprous oxide. The larger the misfits on the surface, the larger would be the number of oxygen ions adsorbed on the surface, leading to high resistance.

(VI) The surface chromination facilitated adsorption of a large number of oxygen ions on the surface, which could immediately oxidize the exposed $H_2S$ gas, leading to faster response of the sensor.

(VII) The fast recovery of the sensor could be attributed to the larger oxygen deficiency in BST. The larger oxygen deficiency would enable BST to adsorb more oxygen ions, helping the sensor to recover fast.

(VIII) Surface chrominated BST was observed to be more sensitive and selective to $H_2S$ gas than cupricated and unmodified BST.

## Acknowledgements

The authors are grateful to the Principal, Pratap College, Amalner, for providing laboratory facilities. Authors are also thankful to the Head, P.G. Department of Physics, Pratap College, Amalner, for his keen interest in this research project. Authors are grateful to Dr U P Mulik, C-MET, Pune, Dr P P Patil, Department of Physical Sciences, N.M. University, Jalgaon and Dr Dharmadhikari, Department of Physics, University of Pune, Pune, for their valuable cooperation rendered for characterizations of the material.

## References

Agarwal S, Sharma G L and Manchanda R 2001 *Solid State Commun.* **119** 681

Aslam M, Chaudhary V A, Mulla I S, Sainkar S R, Mandale A B, Belhekar A A and Vijayamohanan K 1999 *Sensors & Actuators* **A75** 162

Chaudhary V A, Mulla I S and Vijayamohanan K 1999 *Sensors & Actuators* **B55** 127

Haeusler A and Meyer J -U 1996 *Sensors & Actuators* **B34** 388

Herbert J M 1980 *Ferroelectric transducers and sensors* (New York: Gordon and Breach)

Hirschfeld T, Callis J B and Kowalski B R 1986 *Science* **226** 312

Ishihara T, Kometani K, Hashida M and Takita Y 1991 *J. Electrochem. Soc.* **138** 173

Ishihara T, Kometani K, Nishi Y and Takita Y 1995 *Sensors & Actuators* **B28** 49

Jain G H, Patil L A, Wagh M S, Patil D R, Patil S A and Amalnerkar D P 2005 *Sensors & Actuators* **B** (available online)

Jain M, Majumdar S B, Katiyar R S and Bhalla A S 2003 *Mater. Lett.* **57** 4232

Kanefusa S, Nitta N and Haradome M 1985 *J. Electrochem. Soc.* **132** 1770

Kim J G, Cho W S and Park K S 2001 *Mater. Sci. Eng.* **B83** 123

Lantto V and Romppainen P 1988 *J. Electrochem. Soc.* **135** 2550

Lee J D 2002 *Concise inorganic chemistry* (London: Van Nostrand Reinhold) 5th ed., p. 698

Lee J K, Park J S and Hong K S 2002 *J. Am. Ceram. Soc.* **85** 1173

Lee M -S and Meyer J -U 2000 *Sensors & Actuators* **B68** 293

Liao B, Wei Q, Wang K Y and Liu Y X 2001 *Sensors & Actuators* **B80** 208

Li B, Lai P T, Li G Q, Zeng S H and Huang M Q 2000 *Sensors & Actuators* **A86** 208

Mair J 1993 *Solid State Ionics* **62** 105

Manku G S 1984 *Inorganic chemistry* (New Delhi: Tata McGraw Hill) p. 465

Manorama S, Sarala Devi G and Rao V J 1994 *Appl. Phys. Lett.* **64** 3163

Meisuer H and Lampe U 1995 *Sensors & Actuators* **B33** 198

Niranjan R S, Chaudhary V A, Sainkar S R, Patil K R, Mulla I S and Vijayamohanan K 2001 *Sensors & Actuators* **B79** 132

Patil L A and Patil D R 2006 *Sensors & Actuators* **B** (available online)

Patil L A, Wani P A, Sainkar S R, Mitra A, Pathak G J and Amalnerkar D P 1998 *Mater. Chem. Phys.* **55** 79

Patil L A, Wani P A and Amalnerkar D P 1999 *Mater. Chem. Phys.* **61** 260

Roy C, Sharma G L, Bhatnagar M C and Samanta S B 2005 *Sensors & Actuators* **B110** 299

Sarala Devi G, Manorama S and Rao V J 1995 *J. Electrochem. Soc.* **142** 2754

Setter N and Collar E L (eds) 1993 *Ferroelectric ceramics* (Basel: Birkhäuser)

Tamaki J, Maekawa T, Miura N and Yamazoe N 1992 *Sensors & Actuators* **B9** 197

Tamaki J, Shimanoe K, Yamada Y, Yamamoto Y, Miura N and Yamazoe N 1998 *Sensors & Actuators* **B49** 186

Wagh M S, Patil L A, Seth T and Amalnerkar D P 2004 *Mater. Chem. Phys.* **84** 228

Wagh M S, Jain G H, Patil D R, Patil S A and Patil L A 2006 *Sensors & Actuators* **B115** 128

Yamazoe N, Kurokawa Y and Seiyama T 1983 *Sensors & Actuators* **B4** 283

Zhu H, Miao J, Noda M and Okuyama M 2004 *Sensors & Actuators* **A110** 371

Zhu W, Tan O K, Yan Q and Oh J T 2000 *Sensors & Actuators* **B65** 366